4098–4105 *Nucleic Acids Research, 1997, Vol. 25, No. 20*

CD, absorption and thermodynamic analysis of repeating dinucleotide DNA, RNA and hybrid duplexes $[d/r(AC)]_{12}\cdot[d/r(GT/U)]_{12}$ and the influence of phosphorothioate substitution

Christopher L. Clark, Paul K. Cecil, Davinder Singh and Donald M. Gray*

The University of Texas at Dallas, Box 830688, Richardson, TX 75083-0688, USA

Received June 9, 1997; Revised and Accepted August 20, 1997

ABSTRACT

Circular dichroism (CD) spectra and melting temperature (T_m) data for five duplexes containing phosphorothioate linkages were compared with data for four unmodified duplexes to assess the effect of phosphorothioate modification on the structure and stability of DNA·DNA and DNA·RNA duplexes. Nine duplexes were formed by mixing oligomers 24 nt long in 0.15 M K^+ (phosphate buffer), pH 7.0. Unmodified DNA·DNA and RNA·RNA duplexes were used as reference B-form and A-form structures. The CD spectra of the modified hybrids S-d(AC)$_{12}$·r(GU)$_{12}$ and r(AC)$_{12}$·S-d(GT)$_{12}$ differed from each other but were essentially the same as the spectra of the respective unmodified hybrids. They were more A-form than B-form in character. CD spectra of duplexes S-d(AC)$_{12}$·d(GT)$_{12}$ and d(AC)$_{12}$·S-d(GT)$_{12}$ were similar to that of d(AC)$_{12}$·d(GT)$_{12}$, except for a reduced long wavelength CD band. Sulfur modifications on both strands of the DNA duplex caused a pronounced effect on its CD spectrum. The order of thermal stability was: RNA·RNA > DNA·DNA > DNA·RNA > S-DNA·DNA > S-DNA·RNA > S-DNA·S-DNA. Phosphorothioation of one strand decreased the melting temperature by 7.8 ± 0.6°C, regardless of whether the substitution was in a hybrid or DNA duplex. Thermodynamic parameters were obtained from a multistate analysis of the thermal melting profiles. Interestingly, the destabilizing effect of the phosphorothioate substitution appears to arise from a difference in the entropy upon forming the DNA·DNA duplexes, while the destabilizing effect in the DNA·RNA hybrids appears to come from a difference in enthalpy.

INTRODUCTION

Phosphorothioate-modified oligodeoxynucleotides (S-ODNs) have attracted considerable attention because of their potential as antisense inhibitors of gene expression. At least 12 clinical trials using S-ODNs as inhibitors of diseases such as HIV, HPV (human papilloma virus) and cancer are currently underway (1–5). Phosphorothioates, like other modified ODNs (methylphosphonates, alkylphosphonates and α-anomers) show an increased resistance to nucleases which is important in maintaining bioavailability of the antisense oligonucleotide (6). Phosphorothioates are especially important because of their ability, when hybridized to their respective target RNA, to remain active as a substrate for the enzyme RNase H (7). The phosphorothioate modification also retains a negative charge on the DNA backbone, which maintains the solubility of the oligonucleotide in aqueous solution. There is evidence that the ability of RNase H to cleave a DNA·RNA hybrid depends to some degree on the flexibility and structure of the hybrid (8). In addition to simple phosphorothioate modifications, chimeric antisense S-ODNs that combine 2′-*O*-alkyl phosphorothioates (to provide stability) and a minimum of five simple phosphorothioate nucleotides (to retain RNase H sensitivity) have been shown to be effective in cells (9). Therefore, the effects of the phosphorothioate modification on the structure and stability of DNA·RNA hybrids are of considerable interest in the development of antisense molecules.

It has been generally observed that the effect of phosphorothioate modification leads to a decrease in the melting temperature of complexes (duplexes or hybrids) formed with such oligomers (10–13). Kibler-Herzog *et al.* (10) showed that duplexes 14 nt long containing phosphorothioate modifications had decreased stability with respect to unmodified duplexes, as monitored by changes in the melting temperature. Freier *et al.* (11) found that melting temperatures of phosphorothioate-modified DNA·RNA hybrids were reduced compared with unmodified hybrids of analogous sequence but that changes in melting temperature per modification were not necessarily correlated with changes in $\Delta G°$(37°C) per modification. What has not been shown, however, is whether the relative decreases in melting temperature seen in modified DNA duplexes and modified DNA·RNA hybrids arise from the same source, such as a global effect on the structure of the complexes formed as a result of the modification, or stem from different mechanisms depending on whether the structure formed is A-form or B-form in character.

Ratmeyer *et al.* (14) showed that unmodified hybrids with mixed purines and pyrimidines on each strand, d/r(CAAC)$_3$·r/d(GUU/(TT)G)$_3$, have lower melting temperatures

*To whom correspondence should be addressed. Tel: +1 972 883 2513; Fax: +1 972 883 2409; Email: dongray@utdallas.edu

than analogous dsDNA sequences in a buffer of 1 M NaCl, consistent with our present data for alternating purine–pyrimidine sequences 24 nt long in a buffer of 0.15 M K^+ (phosphate). CD spectra presented by Ratmeyer *et al.* (14), using a buffer of 3.75 mM Na^+ (phosphate) and 0.1 M NaCl, and our spectra are consistent in both shape and magnitude.

We have studied nine possible combinations of $[d/r(AC)]_{12}$ plus $[d/r(GT/U)]_{12}$ strands: (1) $d(AC)_{12}{\cdot}d(GT)_{12}$; (2) $S\text{-}d(AC)_{12}{\cdot}d(GT)_{12}$; (3) $d(AC)_{12}{\cdot}S\text{-}d(GT)_{12}$; (4) $S\text{-}d(AC)_{12}{\cdot}S\text{-}d(GT)_{12}$; (5) $r(AC)_{12}{\cdot}r(GU)_{12}$; (6) $r(AC)_{12}{\cdot}d(GT)_{12}$; (7) $d(AC)_{12}{\cdot}r(GU)_{12}$; (8) $r(AC)_{12}{\cdot}S\text{-}d(GT)_{12}$; (9) $S\text{-}d(AC)_{12}{\cdot}r(GU)_{12}$. Five of these have phosphorothioate-modified linkages in one or both strands. The sequences chosen were composed of repeating purine–pyrimidine dinucleotides which minimized the risk of forming alternate structures such as hairpins and triple-stranded structures. The sequences were chosen to be 24 nt long to minimize end effects. DNA·DNA and RNA·RNA duplexes were used as reference A-form and B-form molecules.

MATERIALS AND METHODS

Six sequences, $r(AC)_{12}$, $r(GU)_{12}$, $d(AC)_{12}$, $d(GT)_{12}$, $S\text{-}d(AC)_{12}$ and $S\text{-}d(GT)_{12}$, were synthesized by Oligos Etc. (Wilsonville, OR). Samples were received as the lyophilized ammonium salt and resuspended in distilled deionized water. Each of the single-strand samples was assayed for homogeneity of length by gel electrophoresis on a 20% polyacrylamide–8 M urea gel stained with SYBR® Green II (Molecular Probes, Eugene, OR). All samples showed single bands corresponding to 24 nt full-length products, with the exception of the sequence $r(AC)_{12}$, which could not be detected using SYBR® Green II. Stock solutions were prepared in 2 mM K^+ (phosphate), pH 7.0, and checked for self-complex formation by CD prior to raising the salt concentration to 0.15 M K^+ (phosphate). Extinction coefficients for the single strands were calculated from monomers and dimers at 20°C with the assumption that molar absorptivity is a nearest neighbor property and that the oligomers were single stranded at 20°C (15). Extinction coefficients at 260 nm for the modified ssDNA oligomers were assumed to be the same as for unmodified ssDNA. Complementary sequences were brought to equimolar concentrations (~6×10^{-5} M nucleotides) by addition of 0.15 M K^+ (phosphate buffer, pH 7.0). Concentrations of the single strands were determined by UV absorbance spectroscopy and from the calculated extinction coefficients. To determine whether duplexes could be formed by mixing each complementary pair of oligomers, classical mixing curves were obtained. Mixtures were made between complementary sequences in ratios of 100:0, 80:20, 67:33, 60:40, 50:50, 33:67, 20:80 and 0:100. All mixtures were equilibrated at 5°C for 24 h prior to collecting absorbance, CD and T_m data. Duplex formation was confirmed by the demonstration of break points in both absorbance and CD mixing curves near a 50:50 molar ratio of the mixed strands.

Absorbance spectra from 350 to 210 nm were collected on a Cary-Varian 118 or an OLIS-modified Cary 14 spectrophotometer using 1 cm cuvettes. Data were digitized and collected every 1 nm at 20°C at a scan speed of 30 nm/min. After subtracting baseline spectra, the data were smoothed using a 13 point quadradic-cubic least squares smoothing algorithm (16). Baseline offsets were corrected by subtracting the average of the first 10 data points of the spectrum. Molar absorbance spectra were plotted as ε, in units of $M^{-1}cm^{-1}$, per mol nucleotide.

CD spectra from 320 to 200 nm were collected on a Jasco J500A or a J710 spectropolarimeter using 1 cm cuvettes. Data were collected at 0.1 nm intervals at a scan speed of 20 nm/min at 20°C. Digitized data collected on the J710 instrument were smoothed using a Fourier transform smoothing function provided with the Jasco software. Data collected on the J500A instrument were smoothed using the same method as for the absorbance data. CD spectra are reported as $\varepsilon_L - \varepsilon_R$, in units of $M^{-1}cm^{-1}$, per mol nucleotide.

Melting data were collected on a six cell OLIS-modified Cary 14 spectrophotometer in 1 cm path length Teflon-capped cuvettes. Absorbance data were collected at 1° increments from 20 to 90°C. At each temperature increment the samples were incubated for 3 min prior to data collection, allowing the samples to come to equilibrium. This step was performed to minimize formation of less energetically favorable structures such as internal loops and slipped structures. Absorbance data as a function of temperature were corrected for volume expansion and smoothed with a sliding 13 point quadratic-cubic function (16) prior to derivitization and multistate curve fitting. Because the number of data points included in this smoothing procedure was less than the number of data points in any one inflection in the melting profile, the melting transitions were not broadened by the smoothing function (16). Raw and smoothed melting profile data were graphically overlaid and showed no distortions of the shape or transitions of the melting profiles.

Thermodynamic parameters were estimated for each of the samples by fitting multistate statistical-mechanical and two-state models to each melting profile (17). Equations for the multistate and two-state models were used as derived by Evertsz *et al.* (17), with the exception that the effective molecularity (n_{eff}) was allowed to vary in the calculation of $\Delta S°$. The statistical-mechanical model used in calculation of the thermodynamic parameters is a multistate aligned zipper model. This model describes the system as a population of single strands of chain length N in equilibrium with duplex species in perfect alignment but with a statistically positioned continuous hydrogen bonded segment of $1, 2, \ldots, N-1, N$ base pairs in length (17). The model accounts for end fraying by varying the position of the hydrogen bonded segment (which ranges from 1 to N). Having a hydrogen bonded segment of $N-2$ nucleotides would describe a duplex with 1 bp frayed on each end or a duplex with 2 nt frayed on one end. Loop formation and slipped duplexes were not explicitly accounted for in the model, however, the population distribution calculated for each sequence shows that duplexes with more than four unpaired nucleotides are rare (less than ~4% of the population of duplexes at the T_m). Previous population distribution analysis by Applequist *et al.* (18) using a staggered zipper model showed that for the homo-oligomer sequence $(A^+)_{11}{\cdot}(A^+)_{11}$ the relative population of frayed or shifted duplexes with greater than three unpaired nucleotides was small. Therefore, it did not seem necessary to apply the more complicated staggered zipper model to our data.

The procedure used to obtain thermodynamic parameters involved (i) fitting the multistate and two-state models to the experimental data to generate parameters used in the calculation of $\Delta H°_{VH\ (multistate)}$ and $\Delta H°_{VH\ (two\text{–}state)}$ respectively, (ii) calculation of the effective molecularity (n_{eff}) and (iii) calculation of $\Delta S°$ and $\Delta G°$ using n_{eff}.

The procedure used to fit the multistate and two-state models to the experimental melting profiles was a Marquardt–Levenburg non-linear fitting routine (19). This routine defines a χ^2 merit

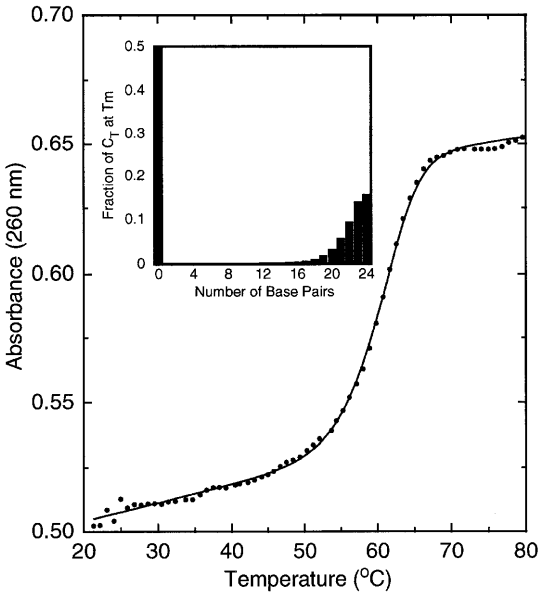

Figure 1. Representative absorbance melting profile of S-d(AC)$_{12}$·d(GT)$_{12}$ in 0.15 M K^+ (phosphate buffer, pH 7.0) fitted by a statistical-mechanical multistate aligned zipper model. The inset graph shows the relative population distribution (as a fraction of the total strand concentration, C_T) of base paired species at a T_m of 60.9°C.

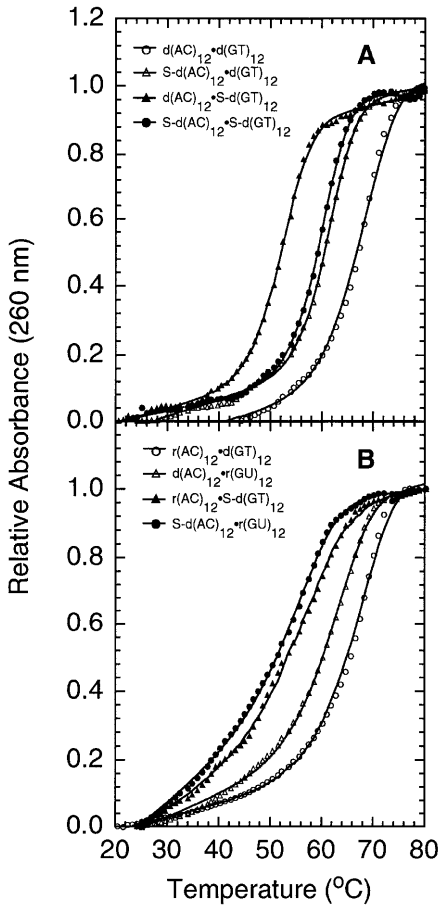

Figure 2. Representative absorbance melting profiles and multistate curve fits for (**A**) modified and unmodified DNA duplexes and (**B**) modified and unmodified DNA·RNA hybrids.

function for the fit of the model to the data and determines best fit parameters by its minimization. Initial estimates for the input parameters were obtained from a manual fit using a spreadsheet. Estimates for the pre- and post-melt regions of the melting profiles were generated by linear regression analysis in the initial stages of program execution for both the two-state and the multistate models. The stopping criterion for the fitting procedure was chosen to be a change in χ^2 of <0.001. To explore the sensitivity of the calculated thermodynamic parameters to the initial estimates used in the model, each melting profile was repeatedly fitted with different input parameters, effectively exploring the topology of the local minima. Although the model is sensitive to the initial input parameters, it was apparent that for each melting profile there was a very limited range of input parameters that gave acceptable χ^2 values. The thermodynamic values generated from the different sets of input parameters for each sample were used to estimate the error in $\Delta H°$ and $\Delta S°$. Input parameters that gave results outside the reported error limits had χ^2 values dramatically higher (>10-fold) than those used in the calculation of the thermodynamic data and were excluded from the analysis.

Values for the effective molecularity for each experiment were obtained by first using the multistate and two-state models to generate parameters used in the calculation of $\Delta H°_{VH\ (multistate)}$ and $\Delta H°_{VH\ (two\text{–}state)}$. Then the effective molecularity (n_{eff}) was set equal to ($\Delta H°_{VH\ (two\text{–}state)}/\Delta H°_{VH\ (multistate)}$ + 1) (20). This effectively absorbs deviations from bimolecular behavior of the melting transition. Plum *et al.* (20) suggest that apparent deviations in molecularity from a value of 2 indicate anomalies in initiation. In any case, varying n_{eff} over the observed range (1.8–2.2) had negligible effect on the values of $\Delta H°_{VH\ (multistate)}$ obtained from the multistate fitting procedure; however, values for n_{eff} different from 2 (1.8–2.2) did have a significant effect on the calculated $\Delta S°$ values. Therefore, n_{eff} was fixed at 2 during the curve fitting procedure but was allowed to vary during the calculation of $\Delta S°$.

Values for $\Delta S°$ were calculated from the equation

$$\Delta S° = \Delta H°_{VH\ (multistate)}/T_{m,s} - R[\ln(2n/C_r)^{(neff\ -\ 1)}],$$

where $T_{m,s}$ was the melting temperature calculated from the multistate curve fit and corrected to a standard strand concentration (C_r) of 1×10^{-6} M. Melting temperatures were determined as the temperature at which half of the double-strand complexes had dissociated, as calculated from the multistate model. Values of $\Delta H°$ and $\Delta S°$ per mol oligomer were then used to calculate $\Delta G°$(37°C). Errors in the fitted parameters are given as the standard deviation of the results of multiple fitting procedures on each sample and were ±2.8 kcal/mol for $\Delta H°_{VH\ (multistate)}$, ±7 cal/(mol·K) for $\Delta S°$ and ±0.3 kcal/mol for $\Delta G°$. Differences in the fitted parameters between repeated samples were typically much smaller than the deviations observed for multiple fittings of the same sample. The covariance of the standard errors in fitted parameters used to calculate $\Delta H°$ and $\Delta S°$ was always <20%.

To compare the melting transitions, the breadth, δT_m (the temperature range of the melting profile over which 80% of the cooperative transition occurred) and the percent hyperchromicity

(the percent increase in absorbance from the beginning to the end of the cooperative transition) were determined for each melting profile.

Population distributions at each temperature along the melting profiles were calculated from data obtained from the multistate fitting procedure using equations 4–7 from Evertsz *et al.* (17). The fraction ($F_{L,T}$) of the total population of oligomers of length N present as duplexes containing a contiguous stretch of base pairs (L) at a given temperature (T) is given by the following equation:

$$F_{L,T} = (1 - \theta_{C,T})(\kappa/q_T)(N - L + 1)s_T^{L-1}$$

In this equation s_T is the equilibrium constant for formation of each successive base pair, q_T is the partition function and $1 - \theta_{C,T}$ is the fraction of strands in the duplex state, where s_T, q_T and $1 - \theta_{C,T}$ are parameters derived from the multistate curve fit. The value of κ (the equilibrium constant for formation of the first base pair) was fixed at 4×10^{-3} (17).

All of the samples investigated showed significant populations of species that had fewer than 24 bp at the T_m, indicating that a simple two-state thermodynamic analysis was not sufficient to describe the melting behavior of these oligomers. A representative melting profile, fitted with the multistate model, and a population analysis are shown in Figure 1. Figure 2 includes representative melting profiles and multistate fits for each of the sequences analyzed.

RESULTS AND DISCUSSION

Absorbance and CD of single strands

Two phosphorothioate-modified and two unmodified single-stranded DNA (ssDNA) oligomers of complementary sequences were mixed with each other or with two complementary RNA sequences to make the nine duplexes listed in Table 1. Molar absorption spectra from 350 to 210 nm of the modified and unmodified ssDNA oligomers are shown in Figure 3. CD spectra from 320 to 200 nm of the ssDNA oligomers are shown in Figure 4.

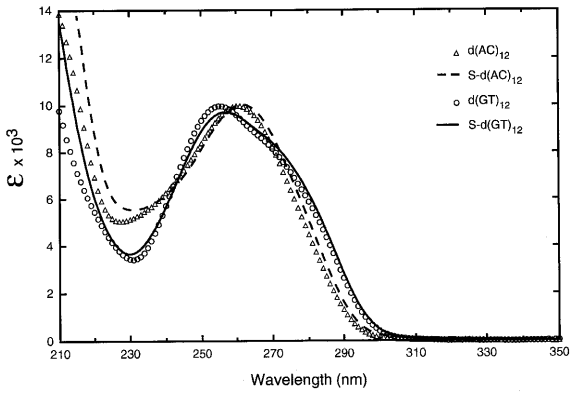

Figure 3. Absorbance spectra of single-stranded oligomers $d(AC)_{12}$ (Δ), S-$d(AC)_{12}$ (– – –), $d(GT)_{12}$ (O) and S-$d(GT)_{12}$ (—). The solution conditions were 0.15 M K^+ (phosphate), pH 7, 20°C for spectra in Figures 2–6.

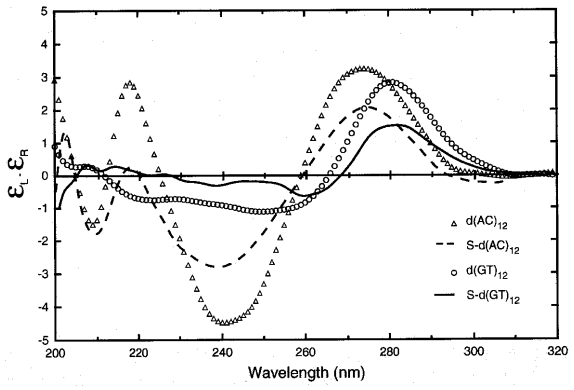

Figure 4. CD spectra of single-stranded oligomers $d(AC)_{12}$ (Δ), S-$d(AC)_{12}$ (– – –), $d(GT)_{12}$ (O) and S-$d(GT)_{12}$ (—).

Table 1. Values of thermodynamic parameters for duplex formation and characteristics of melting profiles for oligomers in 0.15 M K^+ (phosphate buffer, pH 7.0)

Sequence	Multistate			Two-state			Melting profile characteristics		
	$\Delta H°$ (kcal/mol)[a]	$\Delta S°$ [cal/(mol K)][a]	$\Delta G°$(37°C) (kcal/mol)[a]	$\Delta H°$ (kcal/mol)[a]	$\Delta S°$ [cal/(mol K)][a]	$\Delta G°$(37°C) (kcal/mol)[a]	T_m (°C)[a,b]	δT_m (°C)[a,b]	Hyperchromicity (%)[a]
$d(AC)_{12}·d(GT)_{12}$	–97.4	–258	–17.5	–97.9	–259	–17.6	67.5	21	32
$r(AC)_{12}·r(GU)_{12}$	ND[c]	ND[c]	ND[c]	ND[c]	ND[c]	ND[c]	68.9	27	26
S-$d(AC)_{12}·d(GT)_{12}$	–126.4	–348	–18.5	–115.5	–318	–17.0	60.9	16	26
$d(AC)_{12}$·S-$d(GT)_{12}$	–122.3	–339	–17.3	–119.2	–330	–16.9	59.6	17	26
S-$d(AC)_{12}$·S-$d(GT)_{12}$	–114.0	–325	–13.2	–115.7	–327	–14.3	51.8	18	25
$d(AC)_{12}·r(GU)_{12}$	–90.2	–237	–16.7	–79.1	–207	–14.9	63.1	16	27
S-$d(AC)_{12}·r(GU)_{12}$	–75.9	–201	–13.6	–72.6	–192	–13.0	56.3	17	28
$r(AC)_{12}·d(GT)_{12}$	–91.6	–242	–16.5	–97.1	–257	–17.6	66.1	18	24
$r(AC)_{12}$·S-$d(GT)_{12}$	–74.8	–196	–14.1	–66.5	–174	–12.6	56.4	17	26

[a]Results are shown as the average of at least three independent determinations on separately formed samples of the duplexes, except in the case of dsRNA, for which the results are the average of two samples. Standard deviations were ±2.8 kcal/mol for $\Delta H°$, ±7 cal/(mol·K) for $\Delta S°$, ±0.3 kcal/mol for $\Delta G°$, ±0.5°C for T_m, ±1°C for δT_m and ±1.5% for hyperchromicity (see Materials and Methods).

[b]Melting temperatures and δT_m values were determined at a total strand concentration of 2.5×10^{-6} M.

[c]Not determined.

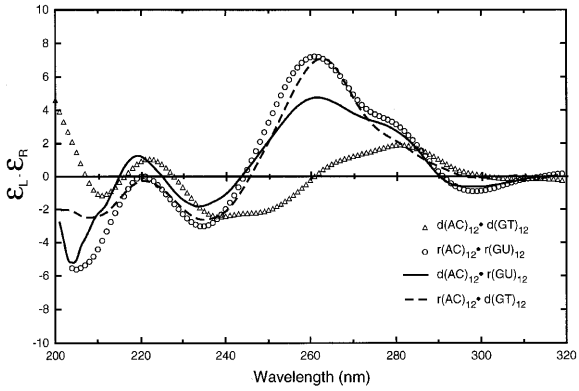

Figure 5. CD spectra of unmodified duplexes $d(AC)_{12}\cdot d(GT)_{12}$ (Δ), $r(AC)_{12}\cdot r(GU)_{12}$ (O), $d(AC)_{12}\cdot r(GU)_{12}$ (—) and $r(AC)_{12}\cdot d(GT)_{12}$ (– – –).

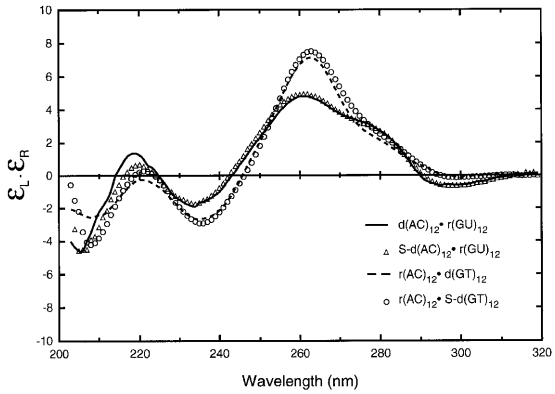

Figure 6. CD spectra of modified and unmodified hybrids $d(AC)_{12}\cdot r(GU)_{12}$ (—), $S\text{-}d(AC)_{12}\cdot r(GU)_{12}$ (Δ), $r(AC)_{12}\cdot d(GT)_{12}$ (– – –) and $r(AC)_{12}\cdot S\text{-}d(GT)_{12}$ (O).

As seen in Figure 3, above 230 nm the absorption spectra of the modified single strands were very similar to the absorption spectra of the corresponding unmodified sequences. In contrast, the measured CD spectra of the single strands in Figure 4 showed significant differences between the modified and unmodified sequences. CD spectra for both modified sequences generally showed decreased band intensities throughout the spectral region from 320 to 210 nm, which indicated that the bases of the phosphorothioate strands were less stacked.

CD of double strand oligomers

CD spectra of $r(AC)_{12}\cdot r(GU)_{12}$, $r(AC)_{12}\cdot d(GT)_{12}$, $d(AC)_{12}\cdot d(GT)_{12}$ and $d(AC)_{12}\cdot r(GU)_{12}$ are shown in Figure 5. The CD spectra for these unmodified oligomer duplexes were very close in band magnitudes and shapes to spectra of their corresponding polymer duplexes at wavelengths above 200 nm (21), which showed that end effects did not significantly affect the spectral features of the oligomeric duplexes. The CD spectrum of the dsRNA $r(AC)_{12}\cdot r(GU)_{12}$ oligomer duplex had negative bands at 300 and below 210 nm and a positive band at 260 nm characteristic of the A-RNA conformation (21,22). The spectrum of the dsDNA $d(AC)_{12}\cdot d(GT)_{12}$ had roughly equal positive and negative bands above 220 nm, with a crossover at 261 nm typical of the B-conformation (23).

There were differences in the CD spectra of the two hybrid oligomers that corresponded to characteristic CD features previously found for the two hybrid sequences (21). Each hybrid also showed both differences from and similarities to the spectrum of the RNA duplex. For example, the strong negative band below 210 nm, present in the spectrum of $r(AC)_{12}\cdot r(GU)_{12}$, was much reduced in the spectrum of $r(AC)_{12}\cdot d(GT)_{12}$, but was about the same magnitude in the spectrum of $d(AC)_{12}\cdot r(GU)_{12}$. In addition, the positive 280 nm shoulder and negative 300 nm band in the $r(AC)_{12}\cdot r(GU)_{12}$ spectrum were not present in the spectrum of $r(AC)_{12}\cdot d(GT)_{12}$, but were present in that of $d(AC)_{12}\cdot r(GU)_{12}$. The spectrum of $d(AC)_{12}\cdot r(GU)_{12}$ was in these respects more similar to that of $r(AC)_{12}\cdot r(GU)_{12}$ than that of $d(AC)_{12}\cdot d(GT)_{12}$, however, the positive band at 260 nm was reduced for $d(AC)_{12}\cdot r(GU)_{12}$ in comparison with this band in the spectra of $r(AC)_{12}\cdot r(GU)_{12}$ or the other hybrid. The latter spectral feature may be a key factor in describing the A-like character of a conformation, since $d(AC)_{12}\cdot r(GU)_{12}$ was the less stable of the two hybrids. On the other hand, the spectral difference between the hybrids may reflect the different strand orientations of the base chromophores in a heteronomous conformation (24 and references therein).

Figure 6 shows the spectra of all four hybrids with and without S-DNAs, $d(AC)_{12}\cdot r(GU)_{12}$, $S\text{-}d(AC)_{12}\cdot r(GU)_{12}$, $r(AC)_{12}\cdot d(GT)_{12}$ and $r(AC)_{12}\cdot S\text{-}d(GT)_{12}$. The spectra of $S\text{-}d(AC)_{12}\cdot r(GU)_{12}$ and $r(AC)_{12}\cdot S\text{-}d(GT)_{12}$ were almost identical to those of the corresponding unmodified hybrids. This showed that the phosphorothioate modification did not significantly affect the different secondary structures of these two types of hybrids.

Figure 7 shows the spectra of the DNA duplexes $d(AC)_{12}\cdot d(GT)_{12}$, $S\text{-}d(AC)_{12}\cdot d(GT)_{12}$, $d(AC)_{12}\cdot S\text{-}d(GT)_{12}$ and $S\text{-}d(AC)_{12}\cdot S\text{-}d(GT)_{12}$. The spectra of $S\text{-}d(AC)_{12}\cdot d(GT)_{12}$ and $d(AC)_{12}\cdot S\text{-}d(GT)_{12}$ were very similar, providing evidence that the structural effect of the phosphorothioate modification was relatively insensitive to which strand contained the modification. However, the CD spectra of both $S\text{-}d(AC)_{12}\cdot d(GT)_{12}$ and $d(AC)_{12}\cdot S\text{-}d(GT)_{12}$ differed from the spectrum of unmodified $d(AC)_{12}\cdot d(GT)_{12}$ in having a decreased positive CD above 260 nm, showing that a phosphorothioate modification of either strand did have an effect on DNA duplex structure. The spectra of $S\text{-}d(AC)_{12}\cdot d(GT)_{12}$ and $d(AC)_{12}\cdot S\text{-}d(GT)_{12}$ are not consistent with A-form, Z-form or condensed Ψ-type duplexes of poly[d(AC)·d(GT)] (25). The decreased long wavelength band is reminiscent of spectra of dehydrated DNAs in a non-standard B conformation (25,26). The spectrum of the duplex with both strands modified, $S\text{-}d(AC)_{12}\cdot S\text{-}d(GT)_{12}$, differed even more significantly from the spectrum of the unmodified DNA. The spectrum of $S\text{-}d(AC)_{12}\cdot S\text{-}d(GT)_{12}$ showed a large decrease in the positive band at 280 nm and the first crossover was red-shifted by 16 nm. These changes above 260 nm may imply a change in the winding angle (26) for DNA duplexes with a phosphorothioate-modified strand. Also, the positive band at 220 nm increased in magnitude in each of the modified DNA duplexes relative to that of the unmodified DNA duplex. This is a feature found for heat-denatured and cooled DNA relative to that of native DNA and may indicate an enhanced intrastrand interaction in the phosphorothioate-modified strands (23).

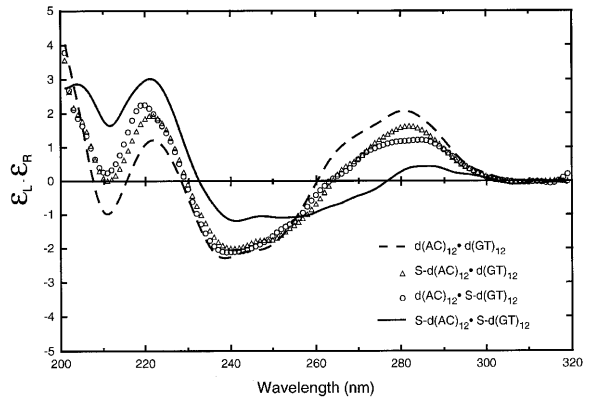

Figure 7. CD spectra of modified and unmodified DNA duplexes $d(AC)_{12}\cdot d(GT)_{12}$ (– – –), $S\text{-}d(AC)_{12}\cdot d(GT)_{12}$ (Δ), $d(AC)_{12}\cdot S\text{-}d(GT)_{12}$ (O) and $S\text{-}d(AC)_{12}\cdot S\text{-}d(GT)_{12}$ (—).

Thermal stability of hybrids and duplexes

The last three columns of Table 1 list the averaged melting temperatures (T_m), δT_m, percent hyperchromicities and thermodynamic parameters for triplicate samples of the nine oligomer duplexes. Melting temperatures for the RNA duplex were slightly less than expected and δT_m values for this duplex were 6–11°C higher than those of the other sequences, which ranged from 16 to 21°C, hinting that there may have been some marginal degradation of the samples of this duplex. Therefore, thermodynamic parameters for the RNA duplex are not included. All of the duplexes showed significant hyperchomicities of 24–32%. Thermodynamic parameters were estimated as described in Materials and Methods. Throughout this work a buffer of 0.15 M K^+ (phosphate buffer, pH 7.0) was used to approximate a physiological salt concentration.

The RNA·RNA duplex had the highest T_m (68.9°C), followed by that of the DNA duplex (67.5°C). The unmodified DNA·RNA hybrid duplexes differed slightly in their T_m values, both of which were lower than the T_m of the DNA duplex. Previously, Gray *et al.* (21) showed that the T_m of poly[r(AC)·d(GT)] was greater than that of poly[d(AC)·r(GU)] by 2°C in a buffer of 0.02 M Na^+ (phosphate, pH 7.0), which is consistent with our data for shorter sequences. Phosphorothioate-modified hybrid duplexes had T_m values lower (6.8 and 9.7°C per strand modified) than those of the corresponding unmodified sequences.

Phosphorothioate-modified hybrids and DNA duplexes had, on average, a T_m decrease of 7.8°C for modification in one strand. The DNA duplex containing modifications on both strands had a T_m reduced by 15.7°C relative to that of the unmodified DNA duplex. The overall order of thermal stabilities for the nine sequences was: r(AC)·r(GU) > d(AC)·d(GT) > r(AC)·d(GT) > d(AC)·r(GU) > S-d(AC)·d(GT) ≈ d(AC)·S-d(GT) > r(AC)·S-d(GT) ≈ S-d(AC)·r(GU) > S-d(AC)·S-d(GT).

Multistate model

Thermodynamic parameters derived from the multistate model are shown in the first three columns of Table 1. The decrease in $\Delta G°$(37°C) for the unmodified hybrids was consistent with the decrease reported by Lesnik and Freier (27) for three hybrid oligomer sequences 15–21 nt long, compared with analogous dsDNA sequences, of 33–80% A+T/U and 50% pyrimidine content, in a buffer of 100 mM Na^+. Thermodynamic analysis of our data revealed that the decrease in melting temperature, although of approximately the same magnitude for modification in one strand in DNA·DNA duplexes and DNA·RNA hybrids, arose from different sources. The effect of phosphorothioation of one strand of a DNA duplex appeared to give rise to a favorable contribution to the enthalpy of formation while effecting the entropy in a very unfavorable manner. The net result of phosphorothioation of the DNA duplex was to increase the stability of the complex at low temperatures (<50°C) and progressively reduce the stability of the complex at increasing temperatures, relative to the unmodified DNA duplex. Thus, at higher temperatures (>50°C) the free energies ($\Delta G°$) of the phosphorothioate duplexes are reduced when compared with the free energies of the unmodified duplexes. This reduction in stability is, in the case of phosphorotioate-modified DNA duplexes, the result of the more unfavorable contribution to entropy. This effect on entropy can be explained if the entropy of the modified single strand is higher than the corresponding unmodified single strand, if the modified duplexes have a lower entropy than the unmodified duplex or if there is a combination of these effects. CD spectra indicated that the modified single strands possess a less ordered structure, which implies that these modified strands may be more flexible and have a higher inherent entropy compared with unmodified DNA. The CD spectra of the modified DNA duplexes also indicated some differences in their structures. Changes in the structure of the modified duplex could reflect an alteration in the order of the water around the backbone of the duplex. Phosphorothioate modification of both strands of a DNA duplex had a pronounced effect on the CD spectra and altered the thermodynamic parameters of this duplex in a fashion similar to that of the DNA duplexes where only one strand was modified. This doubly modified duplex had a slightly more favorable $\Delta H°$, relative to unmodified DNA duplexes, and an unfavorable contribution to entropy, as observed for the DNA duplexes modified in only one strand. In total, the factor dominating the decrease in the stability of the modified DNA duplexes was entropic in character.

In contrast to the effect of phosphorothioation of DNA duplexes, the effect of modifying the DNA strand of DNA·RNA hybrids appeared not to dramatically affect $\Delta S°$ for duplex formation. Both of the modified hybrids showed an unfavorable contribution to $\Delta H°$ and a slighty favorable contribution to $\Delta S°$, the opposite of what was found for DNA duplexes modified in one strand. While CD spectra indicated differences in the structures of the modified DNA duplexes with respect to the unmodified duplexes, the CD spectra of the hybrids and modified hybrids were identical. Gyi *et al.* (28) have shown using NMR that the DNA strand in a DNA·RNA hybrid is more flexible than that in a DNA duplex. It is possible that the modified DNA has the freedom necessary to adopt a structure similar to that of unmodified hybrids. In the case of the modified hybrids the dominant factor in decreasing $\Delta G°$, relative to that of the corresponding unmodified hybrid, is a reduction in $\Delta H°$. These differences in the thermodynamic parameters of the two types of complexes (DNA duplexes and DNA·RNA hybrids) may arise from a combination of factors, including differences in the entropy of the single strands, altered water structure around the backbone of the duplexes and altered stacking interactions.

Two-state model

Thermodynamic parameters derived from a simple two-state model are also shown in Table 1 for comparison. The values of $\Delta G°$(37°C) from this model often differed significantly from those derived from the multistate model. The values of $\Delta H°$ and $\Delta S°$, however, show the same trends as discussed for values derived from the multistate model; i.e. the different enthalpic and entropic contributions from phosphorothioate substitutions in a DNA or hybrid duplex are evident from even this simple model.

CONCLUSIONS

The oligomeric sequences $d(AC)_{12}\cdot d(GT)_{12}$, $r(AC)_{12}\cdot r(GU)_{12}$, $d(AC)_{12}\cdot r(GU)_{12}$ and $r(AC)_{12}\cdot d(GT)_{12}$ exhibited CD spectra that were similar to those of the corresponding polymer sequences, demonstrating that structural parameters inherent to these sequences were preserved in the shorter 24 nt oligomers.

The CD spectra of ssDNA oligomers containing phosphorothioate backbones differed considerably from CD spectra of unmodified DNA oligomers of the same sequence. This effect was alleviated when the modified DNA was hybridized with its complementary RNA and the effect was partially alleviated when hybridized to its complementary DNA. However, when both strands of a DNA duplex contained phosphorothioate modifications, the CD spectrum of the resulting duplex differed markedly from the spectrum of either the unmodified DNA duplex or the DNA duplex containing modifications in one strand. This could result from an increased flexibility in the phosphorothioate-modified DNA strands, such that when one strand is modified the remaining unmodified (either DNA or RNA) strand has a dominant role in determining the structure. Hence, when both strands of a DNA duplex are modified, it is possible that increased flexibility in both strands leads to a structure different from the unmodified duplex. Benimetskaya *et al.* (29) previously suggested that phosphorothioate-modified DNA is more rigid than unmodified DNA because of a proposed reduction in the tetrahedral angle of the bridging O-P-O which could limit the conformational entropy of the oligomer. While the O-P-O angle may be reduced by the presence of the sulfur atom, our data are more consistent with an increase in flexibility of phosphorthioate-modified DNA strands.

Thermodynamic analysis of the modified and unmodified DNA duplexes revealed that the factor driving the reduction in T_m of the modified duplexes was a decrease in $\Delta S°$ for formation of the complex. $\Delta H°$ for each of the modified DNA duplexes with a modification in one strand was greater than that for the unmodified duplexes, indicating that changes induced by the phosphorothioate modification did not adversely effect $\Delta H°$ for formation of the DNA duplexes. Therefore, at 37°C, $\Delta G°$ values for both of the singly modified duplexes were approximately the same as for the unmodified dsDNA. This is an important finding because it has previously been thought that S-DNA would not act as a significant competitor to other dsDNA sequences because it possesses a lower melting temperature. This may not be the case at 37°C at physiological salt concentration.

Phosphorothioate-modified DNA·RNA hybrids $S\text{-}d(AC)_{12}\cdot r(GU)_{12}$ and $r(AC)_{12}\cdot S\text{-}d(GT)_{12}$ had CD spectra very similar to those of the corresponding unmodified hybrids; however, melting temperatures for the modified hybrids were reduced by 6.8 and 9.7°C. It appears that the reduced stability imparted by the phosphorothioate modification did not result from differing duplex conformations induced by the sulfur modification because the CD spectra of these hybrids were very similar to those of the unmodified duplexes. Thermodynamic analysis of the hybrids revealed that although the $\Delta S°$ values for formation of the modified hybrids were slightly more favorable, possibly as a result of differences in the ordering of water around the backbones of the modified and unmodified hybrids, the values for $\Delta H°$ were lower [for both $S\text{-}d(AC)_{12}\cdot r(GU)_{12}$ and $r(AC)_{12}\cdot S\text{-}d(GT)_{12}$] than those of the unmodified hybrids. Therefore, in the case of DNA·RNA hybrids the factor driving the reduction in T_m of phosphorothioate-modified hybrids was a decrease in $\Delta H°$ and not a decrease in $\Delta S°$ as in the case of the DNA duplexes.

In summary, the effect on the structure and stability of complexes formed with phosphorothioate-modified DNA differed depending on the nature of the complementary strand. In a complex with another DNA strand, phosphorothioate-modified DNA altered the structure, as determined by CD spectroscopy, relative to that of unmodified DNA duplexes of the same sequence, and lowered the melting temperature by decreasing $\Delta S°$ for the reaction. On the other hand, phosphorothioate-modified DNA in a complex with a complementary RNA strand did not alter the structure, compared with that of the unmodified hybrid of the same sequence, and lowered the T_m by decreasing $\Delta H°$. At physiological salt concentration, T_m values of the modified hybrids were decreased by about the same magnitude as were the T_m values of the DNA duplexes modified in one strand, but were mediated by different mechanisms.

ACKNOWLEDGEMENTS

This work was performed by C.L.C. in partial fulfillment of the requirement for the PhD degree in the Department of Molecular and Cell Biology, the University of Texas at Dallas. We thank Dr Scott Law (Chemistry Department, Rutgers University) for helpful discussions and review of this manuscript. Support was provided by grants from the Texas Advanced Technology Program (grant no. 9741-036), Cytoclonal Pharmaceutics Inc. (Dallas, TX) and the Robert A.Welch Foundation (grant AT-503).

REFERENCES

1 Glazer,V. (1996) *Genet. Engng News*, **16**, 1–21.
2 Zhang,R., Yan,J., Shahinian,H., Amin,G., Lu,Z., Liu,T., Saag,M.S., Jiang,Z., Temsamani,J., Martin,R.R., Schechter,P.J., Agrawal,S. and Diasio,R.B. (1995) *Clin. Pharm. Ther.*, **58**, 44–53.
3 Crooke,S.T., Grillone,L.R., Tendolkar,A., Garrtet,A., Fraktin,M.J., Leeds,J. and Barr,W.H (1994) *Clin. Pharm. Ther.*, **56**, 641–646.
4 Bayever,E., Iversen,P.L., Bishop,M.R., Sharp,J.G., Tewary,H.K., Ameson,M.A., Pirruccello,S.J., Ruddon,R.W., Kessinger,A., Zon,G. and Armitage,J.O. (1993) *Antisense Res. Dev.*, **3**, 383–390.
5 Matteucci,M.D. and Wagner,R.W. (1996) *Nature*, **384**, 20–22.
6 Piegra,J.-Y. and Magdelenat,H. (1994) *Mol. Cell. Biol.*, **40**, 237–261.
7 Rothenberg,M., Johnson,G., Laughlin,C., Green,I., Cradock,J., Sarver,N. and Cohen,J.S. (1989) *J. Natl. Cancer Inst.*, **81**, 1539–1544.
8 Oda.Y, Iwai,S., Ohtuska,E., Ishawa,M., Ikehara,M. and Nakamura,H. (1993) *Nucleic Acids Res.*, **21**, 4690–4695.
9 Monia,B.P., Lesnik,E.A., Gonzalez,C., Lima,W.F., McGee,D., Guinosso,C.J., Kawasaki,A.M., Cook,P.D. and Freier,S.M., (1993) *J. Biol. Chem.*, **268**, 14514–14522.

10 Kibler-Herzog,L., Zon,G., Uznanski,B., Whittier,G. and Wilson,W.D. (1991) *Nucleic Acids Res*., **19**, 2979–2986.
11 Freier,S.M., Lima,W.F., Sanghvi,Y.S., Vickers,T., Zounes,M., Cook,P.D. and Ecker,D.J. (1992) In Erickson,R.P. and Izant,J.G. (eds), *Gene Regulation: Biology of Antisense RNA and DNA*. Raven Press, New York, NY, pp. 95–107.
12 Kandimalla,E.R., Manning,A., Zhao,Q., Shaw,D.R., Byrn,R.A., Sasisekharan,V. and Agrawal,S. (1997) *Nucleic Acids Res*., **25**, 370–378.
13 Cummins,L., Graff,D., Beaton,G.F., Marshall,W.S. and Caruthers,M.H. (1996) *Biochemistry*, **35**, 8724–8741.
14 Ratmeyer,L., Vinayak,R., Zhong,Y.Y., Zon,G. and Wilson,D. (1994) *Biochemistry*, **33**, 5298–5304.
15 Hung,S.H., Yu,Q., Gray,D.M. and Ratliff,R.L. (1994) *Nucleic Acids Res*., **22**, 4326–4334.
16 Savitzky,A. and Golay,M.J.E. (1964) *Anal. Chem*., **36**, 1627–1639.
17 Evertsz,E.M., Karsten,R. and Jovin,T.M. (1994) *Nucleic Acids Res*., **16**, 3293–3303.
18 Applequist,J. and Damle,V. (1965) *J. Am. Chem. Soc*., **87**, 1450–1458.
19 Press,W.H, Teukolsky,S.A., Vetterling,W.T. and Flannery,B.P. (1992) *Numerical Recipes in C*, 2nd Edn. Cambridge University Press, New York, NY, pp. 683–688.
20 Plum,E.G., Grollman,A.P., Johnson,F. and Breslauer,K.J. (1995) *Biochemistry*, **34**, 16148–16160.
21 Gray,D.M. and Ratliff,R.L. (1975) *Biopolymers*, **14**, 487–498.
22 Gray,D.M., Liu.J.-J., Ratliff,R.L. and Allen,F.S. (1981) *Biopolymers* , **20**, 1337–1382.
23 Gray,D.M., Ratliff,R.L. and Vaughan,M.R. (1992) *Methods Enzymol*., **211**, 389–406.
24 González,C., Stec,W., Kobylanska,A., Hogrefe,R.I., Reynolds,M. and James,T.L. (1994) *Biochemistry*, **33**, 11062–11072.
25 Vorlícková,M. (1995) *Biophys. J*., **69**, 2033–2043.
26 Johnson,C.W. (1996) In Fasman,G.D. (ed.), *Circular Dichroism and the Conformational Analysis of Biomolecules*. Plenum Press, New York, NY, pp. 433–465.
27 Lesnik,E.A. and Freier,S.M. (1995) *Biochemistry*, **34**, 10807–10815.
28 Gyi,J.I., Conn,G.L., Lane,A.N. and Brown,T. (1996) *Biochemistry*, **35**, 12538–12548.
29 Benimetskaya,L., Tonkinson,J.L., Koziolkiewicz,M., Karwowski,B., Guga,P., Zeltser,R., Stec,W. and Stein,C.A. (1995) *Nucleic Acids Res*., **23**, 4239–4245.